Dislocation Etch Pits in Quartz

S. L. Brantley, S. R. Crane, D. A. Crerar, R. Hellmann, and R. Stallard

Department of Geological and Geophysical Sciences, Princeton University, Princeton, NJ 08544

Quartz samples were etched hydrothermally at 300°C in etchants of controlled Si concentration to measure the concentration above which dislocation etch pits would not nucleate. The C_{crit} for 300°C was predicted to be $0.6C_o$ and the measured C_{crit} was $0.75C_o \pm .15$ (C_o = equilibrium concentration). Our observations suggest that for $C > C_{crit}$, dissolution occurs at edges and kinks on the surface; while for $C < C_{crit}$, dislocation etch pits form rapidly, contributing to the overall dissolution rate. Analysis of quartz particles from a soil profile revealed a transition from angularly-pitted grain surfaces at the top to rounded surfaces at the bottom, suggesting that downward permeating fluids pass through the critical Si concentration. The theory of etch pit formation may be useful in interpreting the chemical conditions of low temperature mineral-water interactions.

Dissolution of a crystal surface is initiated at sites of high surface energy: edges, corners, cracks, scratches, and holes are favorable sites for fast dissolution. At the micro-scale, trapped impurities, point defects, twin boundaries, and dislocations can also cause enhanced dissolution. The formation of etch pits by dissolution at dislocations has been of particular interest to experimentalists interested in testing and developing theories of dissolution, lattice strain, and material deformation. Frank (1), Cabrera, et al. (2), and Cabrera and Levine (3) developed the first theory of etch pit formation based on dislocation lattice strain. Experiments by Sears (4), Gilman, Johnston and Sears (5), and Ives and Hirth (6) showed that these simple theories appeared consistent with dissolution of LiF. Lasaga (7) recently pointed out implications for interpretation of dissolved mineral surfaces and paleofluid histories. Several types of experiments are suggested by these theories which apply to geochemical processes such as hydrothermal alteration, weathering, and other dissolution reactions.

We describe here an experiment which indicates that the dislocation etch pit theory is a useful tool in interpreting formation of

0097-6156/86/0323-0635$06.00/0

etch pits in quartz by hydrothermal dissolution. We have also tested the theory by documenting the incidence of etch pits on surfaces of quartz grains sampled from a soil profile. Finally, we discuss other approaches suggested by our experiments and by experiments in the literature which would provide useful geochemical information about the rates and mechanisms of natural dissolution processes.

Theory of Etch Pit Formation

Pit formation. If we consider a dissolution nucleus at a screw dislocation intersecting the surface which consists of a cylindrical hole of radius r, one atom layer deep (a), then the free energy of formation of this nucleus will be composed of a volume energy, surface energy, and elastic strain energy term, respectively, as follows:

$$\Delta G = \pi r^2 ag + 2\pi r a\gamma - a\tau b^2(\ln(r/r_o))/4\pi \qquad (1)$$

where τ is the shear modulus, b is the Burger's vector, r_o is the dislocation core radius, γ is the surface energy, and g is the free energy of dissolution per unit volume (2,3). Equation 1 shows that opening of a pit on a crystal surface is a competition between terms which decrease the free energy (dissolution of a volume of crystal into an undersaturated medium and release of dislocation strain energy) and a term which increases the free energy (creation of additional surface area). The cylindrical hole geometry is chosen for simplicity. To predict whether an etch pit will form at a dislocation, we want to determine the variation of ΔG with radius, r, and free energy of dissolution, g, defining g as the chemical affinity per unit volume and neglecting activity corrections:

$$g = RT \ln(C/C_o) / V \qquad (2)$$

where C = concentration of dissolving species, C_o = equilibrium solubility of the species, V is the molar volume, R is the gas constant and T is the absolute temperature. Equation 1 expresses the free energy in enlarging the pit from a radius r_o to a radius r. The core radius, r_o, is the radius of the central volume of the dislocation where the continuum approximation breaks down and electronic energies become important. For $r < r_o$, the elastic strain term of Equation 1 cannot adequately predict the dislocation energy. Because the nature and energetics of the dislocation core are not well understood, the value of r_o is undetermined, and we have chosen to set r_o = b, following other workers (8). For quartz at 300°C, using a shear modulus of 0.48×10^{11} Pa (9), a Burger's vector of 7.3 A (9), a surface energy of 360 mJm^{-2} (10), and a molar volume of 22.688 cm^3, we can calculate ΔG as a function of r for different values of the saturation index, C/C_o. In Figure 1 we have plotted calculated values of ΔG as a function of r (> r_o) and C for a pit one molecule deep in quartz at 300°C, a temperature where quartz readily dissolves in water. Lettered curves correspond to the following concentrations: A (0.04C_o), B (0.36C_o), C (0.51 C_o), D (0.64C_o), E (0.73C_o), F (0.82C_o), G (0.89C_o). Concentrations were chosen to correspond to selected experimental run conditions. Note that all calculations have used Equation 1, which is strictly valid

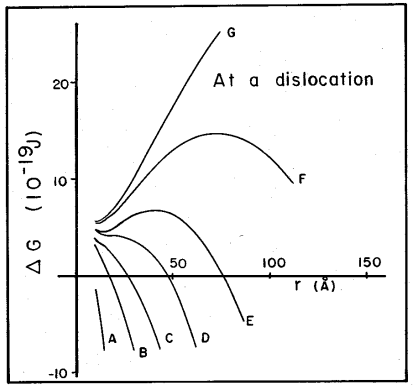

Figure 1. Calculated values of ΔG, free energy of formation of a pit at a dislocation on a quartz surface at 300°C, plotted vs. pit radius, r. Labels defined in text. Adapted with permission from Ref. 16. Copyright 1986 Pergamon Press.

only for screw dislocations. For edge dislocations, the strain energy term is modified by the factor $(1/(1-\nu))$ where ν is Poisson's ratio. For quartz, $\nu = 0.077$, and the correction is very small.

As Figure 1 shows, all the calculated ΔG curves above curve D show a minimum (very near to r = 10 Å) and a maximum (at large values of r_o) in the free energy. The critical concentration where the minimum and maximum in the ΔG curve disappear can be determined by maximizing ΔG with respect to r and solving for r (2,3):

$$r = (-\gamma/2g)[1 \pm (1 - \tau b^2 g/2\pi^2\gamma^2)^{1/2}] \quad (3)$$

Values of r satisfying Equation 3 (corresponding to the minimum and maximum points in ΔG) will yield steady state solutions where a pit radius should remain constant, while the rest of the crystal grows or dissolves depending on the chemical affinity (Equation 2). If the term $\tau b^2 g /2\pi^2\gamma^2 > 1$, there are no real solutions to Equation 3 and there is no steady state value of r, which indicates that a small pit nucleated at a dislocation core should spontaneously open up to form a macroscopic etch pit. The critical concentration at which this occurs (setting the above term equal to one) is :

$$C_{crit} = C_o \exp(-2\pi^2\gamma^2 V/RT\tau b^2) \quad (4)$$

For $C = C_{crit}$, there is a double root to the maximization equation, and there is an inflection point in the ΔG function (curve D on Figure 1). Since there is no activation barrier to opening up the etch pit, any pit nucleated at a dislocation should open up into a macroscopic etch pit. Similarly, for $C < C_{crit}$, there are no real solutions and no maxima and minima in the ΔG function, and nucleated pits open up into etch pits. At 300°C, the calculated C_{crit} for quartz equals $0.6C_o$.

Above C_{crit} (i.e. E or F in Figure 1), there are two real roots to the equation, so there is a minimum and a maximum in the ΔG function. If a pit is nucleated at the core, the pit should spontaneously open until its radius fulfills the condition that ΔG is at a minimum (~10 Å). There is then an activation barrier ΔG^* ($=\Delta G_{maximum} - \Delta G_{minimum}$) toward further opening of the pit into a macroscopic etch pit. Monte Carlo simulations of etch pit formation have shown that such hollow tubes should be stable for some materials, including quartz (27). Above C_{crit}, the height of the activation barrier (ΔG^*) will determine the rate of formation of etch pits. If metastable equilibrium is assumed for the pit nuclei size distribution, the rate of formation of pits per unit area, J, for concentrations above critical should have the form:

$$J = X_d A \exp(-\Delta G^*/RT) \quad (5)$$

where X_d is the fraction of surface sites intersected by dislocations, and A is a frequency factor (11). If the core energy is included in the ΔG calculation, a small activation barrier exists even for pit nucleation below C_{crit}. Pit nucleation in highly undersaturated solutions should then also show a rate dependence as in Equation 5, with a substantially smaller activation energy.

Dissolution kinetics at etch pits. If an etch pit opens up at a dislocation, the slope of the sides of the pit, determined by the ratio of downward dissolution rate v_n to outward dissolution rate v_s, must be high in order for the etch pit to be microscopically observable. If the crystal surface is close-packed, then holes nucleated in the close-packed surface will consist of high-index faces composed of stepped ledges. Anisotropy of v_s will cause etch pits to have crystallographically-controlled non-cylindrical geometries. The rate v_n is the rate of formation of holes at a dislocation, and the rate v_s is the ledge velocity or the rate of recession of ledges away from the nucleated holes. Kinks in the ledges serve as sites of easiest transfer of molecules from the surface into solution. Johnston (12) suggested that the ratio $v_n/v_s > 0.1$ for an etch pit to be microscopically visible.

When v_n is small compared to v_s, ledge spacing at the apex of the nucleated pit will be large, and as the ledges recede, the walls of the pit will be maintained at a very shallow angle, making the pit unidentifiable. Sears and co-workers (4,5) pointed out that the adsorption of poisons onto the dissolving pit surface can decrease v_s, producing a more visible pit. Based on observed etching on etching in LiF, they concluded that poisons were essential for the formation of etch pits on crystal surfaces. The importance of poisons in the formation of etch pits in other substances needs to be investigated.

Etch Pits in Quartz: A Test of the Theory

Hydrothermal etching. To test the prediction of a critical concentration in etch pit formation, we investigated the hydrothermal dissolution of quartz. Previous workers (13,14) noted two types of triangular etch features, deep pyramidal pits and shallow flat pits, produced by hydrothermal etching with distilled water on the rhombohedral face. These workers argued that the shallow flat pits correspond to surface defects while the deeper pits correspond to dislocations. Because of the background work completed on dislocation etch pits on rhombohedral faces of quartz, we decided to investigate etching on this surface.

We ran two different types of dissolution experiments: closed and flow. For the closed experiments, we placed cut pieces of Arkansas quartz with 50 ml of silica solution (prepared according to the method of Crerar et al., (15) and neutralized to pH 7 with NaOH) in standard sealed autoclaves in a temperature-controlled oil bath. In each experiment, all pieces were cut from one face of a large crystal. Different crystals, all of the coarse-crystallized variety from Hot Springs, Arkansas, were used for each run. Dissolution was allowed to proceed for 6.5 hours at 300°C at saturated vapor pressure. Heat up time was from 3-5 hours, and silica concentration during the run usually increased to supersaturated conditions. In the flow experiments, quartz was placed in a flow-through chemical reactor at 300°C (heat up time approximately 30 minutes), and a Si solution of known concentration was pumped through at a rate of 0.7 ml/min at saturated vapor pressure. Solution chemistry was monitored throughout the run. After the experiment, etching on the crystal face was analyzed by SEM.

Specific experimental run conditions and observations are described in Brantley et al. (16). In order to quantify the presence of

etch pits, pit density counts were made for most samples. Fifteen to forty surface samples were randomly selected and imaged at 1000x under SEM, and deep pyramidal pits were counted. Pit densities are plotted in Figure 2, along with the calculated critical concentration. Error bars (see 16) are liberal estimates of statistical counting error and the systematic error involved in distinguishing etch pits. A least squares linear fit to the data from each individual crystal face is plotted in order to estimate the C_{crit} where pit densities reach background levels.

For all runs, there is a clear decrease in measured pit density with increasing C/C_o ratio. In the closed experiments, pit densities reach background levels ($<3 \times 10^3$ cm^{-2}) at $C/C_o = 0.75$. In the flow experiments, samples from crystal R5 (etched for 6.5 hours) and R5SE (crystal R5 after etching 6.5 hours cleaned and re-etched for 25 more hours) show background levels (1×10^4 cm^{-2}) above $C/C_o = 0.8$. Figure 3 shows R5SE surfaces etched above and below 0.8 C_o.

Crystal R9, whose unreacted surface was rougher and more disturbed than the R5 surface, shows a significant decrease in pit density between $C/C_o = 0.75$ and 0.89. Extrapolating the limited R9 data to background pit density ($\sim 2 \times 10^3$ cm^{-2}) predicts $C_{crit}/C_o = 0.9$. Although formation of etch pits decreased markedly above $0.75C_o$ for R9, some etch pits still formed at $C/C_o = 0.9$. In addition, crystal R9 showed considerable "arcuate etching", a general term which describes a variety of unusual etch features common to quartz: curved etch lines, elongated etch triangles, and linear arrays of etch lines and etch triangles, usually with curved edges (16,17). These features could be associated with surface scratches, high impurity content, inclusions, or other flaws disturbing the surface. TEM analysis of samples R5 and R9 indicated that dislocation densities were similar in the two crystals; therefore, heightened etching of R9 might be attributed to segregated impurities which perturb the surface energy of the R5 or R9 dislocations. Alternatively, increased etching might result from differences in Burger's vectors or the screw or edge character of the two crystals' grown-in dislocations. The presence of disturbed surface layers on some crystals of natural quartz was also noticed in the etching experiments of Hicks (17).

Our best estimate from the experimental data in Figure 2 for C_{crit} at 300°C is .0078 ± .0007 m Si which corresponds to 0.8 (± 0.07) C_o. However, we have used Walther and Helgeson's (18) value of 0.0097 m Si as the best value for the equilibrium concentration, C_o. If we use Fournier and Potter's (19) value of 0.011m Si for C_o, then our experimental $C_{crit} = 0.7C_o$, which is closer to the theoretically predicted C_{crit} of $0.6C_o$. Because of the uncertainty in C_o and the uncertainty in our data, our best experimental estimate is $C_{crit} = 0.75 \pm .15\ C_o$ at 300°C.

A very accurate measurement of C_{crit} would allow back-calculation of the surface energy for a given crystal. Because C_{crit} is dependent on the square of γ, such a measurement could be a very sensitive method of measuring interfacial energy at dislocation outcrops. The calculated interfacial energy from our experiments is 280± 90 mJm^{-2} for the rhombohedral face of quartz at 300°C. Parks (10) estimated 25°C value of 360 ± 30 mJm^{-2} is well within the experimental error of our measurement. The best way to determine the value of C_{crit} would be to measure etch pit nucleation rate on

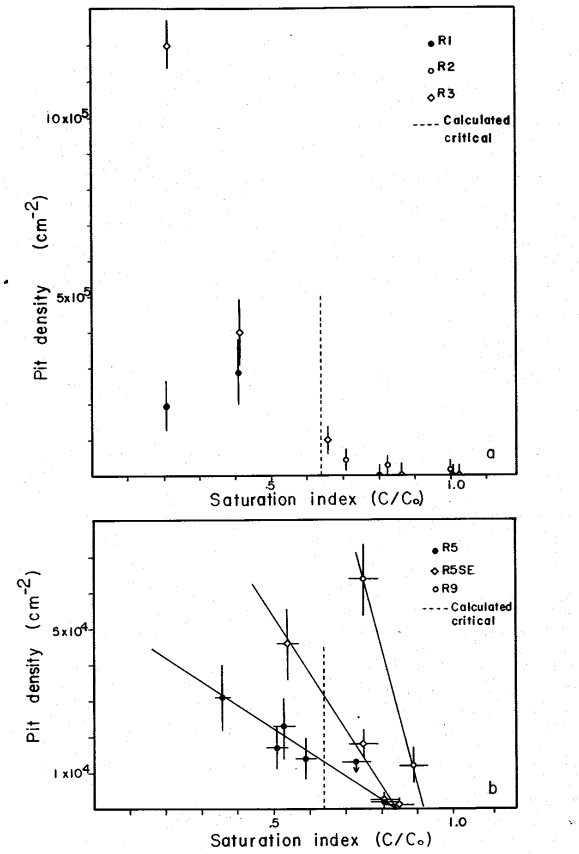

Figure 2. The effect of dissolved Si concentration on etch pit density on quartz surfaces etched: a) in sealed autoclaves for 6.5 hours, b) in a flow reactor for 6.5 hours (R5), 31.5 hours (R5SE), and 25-28 hours (R9). Reproduced with permission from Ref. 16. Copyright 1986 Pergamon Press.

one surface under different silica concentrations. By plotting log (rate) vs. log $(C/C_o)^{-1}$ as suggested by Equation 5, a break in slope should occur at C_{crit} regardless of the dislocation density of the starting material.

Low temperature etching. Our data suggests that, under hydrothermal conditions the rate of pit formation is dramatically reduced, although perhaps not completely stopped, at $C = C_{crit}$. Etch pits on a natural, hydrothermally-etched quartz surface therefore indicate extended dissolution times, but not necessarily etching at $C < C_{crit}$. This is because the rate of etch pit formation even above C_{crit} can be significant at elevated temperatures (as shown by crystal R9). However, at low temperatures, formation of etch pits when $C > C_{crit}$ would be less likely, and natural surfaces etched at low temperature should record the saturation state of the etching fluid.

In order to test this hypothesis, Crane (20) analyzed the surfaces of quartz grain samples from a 90 cm deep soil profile developed in situ on the Parguaza granite, Venezuela (21). Figure 4 shows characteristic surface morphologies from sand grains from just above granite bedrock (90 cm deep) and from 50 cm above bedrock (40 cm deep). As suggested by this figure, a transition occurs at a depth between 60 and 80 cm from angularly-pitted surfaces to rounded surfaces, suggesting that the critical concentration is reached at that point. These observations suggest that, at 25°C, rates are slow enough that for $C > C_{crit}$, no etch pit formation occurs.

Based on predicted weathering and erosion rates of the region, we estimate the profile to be several million years old. Because the soil has developed in situ, the topmost grains have reacted with water for the greatest extent of time. With depth, the total "lifetime" of the particles as soil decreases. This implies that the topmost quartz surfaces should be "reactively mature" (all fines removed, deep grown-together etch pits) and the bottom-most quartz surfaces should be "reactively young" (plentiful fines, fresh surfaces).

Reactively young surfaces in contact with undersaturated solutions should show high rates of pitting. The lack of pitting in bottom samples suggests that the critical Si concentration in the permeating fluid has been exceeded and etch pits are not forming at significant rates. Modeling (21), corroborated by the observation of rounded grain shapes observed in bottom-most layers, indicates ongoing quartz dissolution. Apparently, dissolution of quartz continues in this zone by dissolution of fines, edges, cracks, etc., but without the formation of etch pits. At a slightly higher zone of the profile, reactively young surfaces are exposed to solutions with $C < C_{crit}$. At this point in the profile, "reactively young" quartz meets very reactive solution, and aggressive quartz dissolution and pitting occurs (Figure 4b). Topmost quartz grains show deep, angular, grown-together pits as expected (16).

Rates of Pit Growth. Joshi and Vag (14) measured the rate of etch pit growth in quartz at several temperatures in a concentrated NaOH solution. They report that the rate of dissolution normal to the surface, v_n, is 0.09 micron/min at 200°C, 0.10 micron/min at 250°C, and 0.12 micron/min at 275°C, and 0.166 micron/min at 300°C. By assuming as a first approximation that precipitation into a disloca-

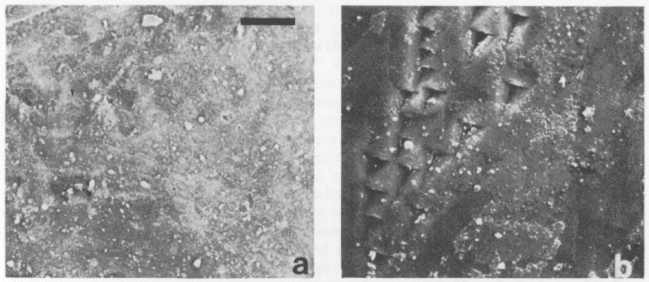

Figure 3. SEM photomicrograph of surfaces of R5SE: a) R5S1SE etched 31.5 hours at 0.008 m Si, b) R5S3SE etched 31.5 hours at 0.006-0.007 m Si (Scale bar = 10 microns).

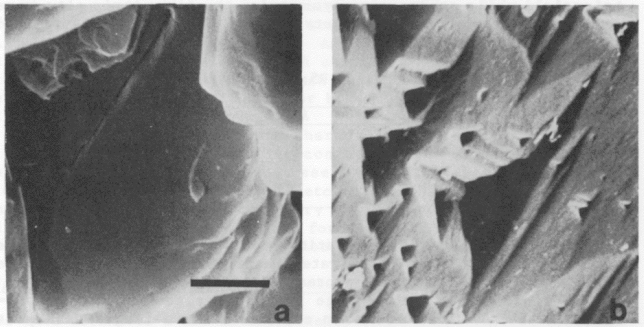

Figure 4. SEM photomicrograph of characteristic surfaces of sand grains from a Venezuelan soil profile. Samples from: a) 90 cm deep, b) 40 cm deep. (Scale bar = 2.5 microns).

tion pit is zero throughout the experiment, we can assume that v_n is directly proportional to the rate constant for dissolution at a dislocation. By regressing ln (v_n) vs. (1/T) for this data, we can estimate an activation energy for this dissolution process at high pH: E_a = 13 kJ/mol. As expected, this activation energy is smaller than the activation energy for dissolution of bulk quartz in water determined for 0°C to 300°C (E_a = ~70kJ/mol, 22) at near-neutral pH. It is interesting to note that this former activation energy is of the same order of magnitude as that measured by Rimstidt and Barnes. Since dissolution at a dislocation has a smaller activation energy than that measured for bulk quartz, pit formation is probably not the rate-limiting step for hydrothermal quartz dissolution. Further experiments on etch pit kinetics are clearly necessary in order to conclusively interpret bulk dissolution data.

Although we did not measure the rate of pit deepening, we did measure the width of etch pits produced on the quartz etched in the flow systems. Pits were imaged by SEM and the small dimension of the etch triangle was measured. By comparing pit widths from crystal R5 etched for 31.5 hours in different Si concentrations, we can compare pit growth rates for different C/C_o values. Pit widths for crystal R5, along with Si concentration of flowing fluids, are tabulated in Table I. We observed a fairly broad variation in pit size for each sample. In particular, we observed that some pits were asymmetric (the deepest etch point off-center from the broader triangle), while others were symmetric; the asymmetric pits were generally smaller than the symmetric pits. Pit symmetry is related

Table I. Crystal R5: Etch Pit Widths

Sample	Si Concen.	Average pit width	Etch time
R5S1SE	0.008 m	1.5 ± .5 microns	31.5 hours
R5S2SE	0.007-.008 m	4.4 ± .9	31.5 hours
R5S3SE	0.006-.007 m	5 ± 2	31.5 hours
R5S5SE	0.005 m	6 ± 2	31.5 hours

to the angle between the dislocation line and the surface as well as the anisotropy of dissolution rate. Despite the uncertainty in the data, there is a noticeable decrease in rate with increasing C/C_o. In addition, the largest change in growth rate occurs above $C = C_{crit}$ (~0.8 C_o). Etch pits on crystal R9 were larger than pits observed on R5. Apparently, whatever surface feature of R9 causes enhanced formation of pits also causes increased rates of pit widening.

Ives and Hirth (6) report similar data for etch pits in LiF, in which the rate of pit widening drops to 0 at $0.22C_o$ and 32°C in dilute ferric fluoride solution, where the 2.5 ppm Fe^{3+} acts as a dissolution poison. They argue that, when no poison is present, the rate should decrease linearly with increasing C/C_o, until the rate equals 0 at $C = C_o$. In the presence of a poison adsorbed to a kink, however, dissociation of a molecule should be slowed, reducing the local equilibrium concentration to a value of $C' < C_o$. If poison molecules completely cover the kink sites, the rate of pit widening could reach 0 at C' rather than C_o. The contribution of poisons to

formation of etch pits in quartz is unclear. In our experiments, we observed that etch pits formed during closed runs were better defined than those of the flow experiments, which could be related either to the higher Na content of the closed run solutions or to the flow conditions. We also tested for Fe content in the flow samples and found less than 1 ppm Fe.

Etch Tubes and Terraced Pits. One interesting feature we observed in some long quartz dissolution experiments was the development of very deep etch holes centered on triangular pits. Hicks (17) has also reported these features. Figure 5 shows an example from sample R5S5SE etched 31.5 hours at 0.5 C_o. Notice that the shape of the etch hole is distinctly different than the larger, triangular etch figure. We believe these features are examples of etch tubes, first noted by Nielsen and Foster (23) in both synthetic and natural quartz etched in 48% HF. These features document conditions such that v_n, rate of pit deepening, is very large. They are thought to be characteristic of quartz dislocations with segregated impurities. Apparently, v_n can be changed quite dramatically by dislocation impurity content. The change in etch hole shape could also be due to impurities in the quartz. Formation of extremely large, widely-spaced etch holes as observed in feldspar (25), and in quartz (26), may also be related to impurity or inclusion content of the crystal. Figure 5 also shows another feature previously described for etched amethyst crystals (24): terraced etch pits. Terraced etch pits are those in which continued dissolution reveals that the dislocation line has a stepped configuration. As the pit deepens, the dislocation line jogs or branches, which causes the center of dissolution to move from the center of the etch triangle. Several examples of etching along apparently stepped or branching dislocations are shown in Figure 5.

In general, the shape and character of etch pits may reveal information about the impurity content of the crystal. "Beaked pits" (pits with curved apexes, see 12) can indicate impurity haloes. Some forms of the arcuate etching we observed in quartz (16) may be examples of beaking. Very shallow pits can form at aged dislocations while very deep pits form at new dislocations. "Aging" may be related to impurity diffusion in the crystal lattice.

Conclusions and Implications for Future Research

We have described a set of experiments which suggests that the etch pit formation theory developed by Cabrera and Levine (2,3) and Frank (1) works well in predicting hydrothermal etching of quartz. Our work shows that at 300°C there is a critical concentration (0.75 ± 0.15 C_o) above which the rate of etch pit formation slows dramatically. We also reported qualitative observations of surface features of quartz sand grains from a 90 cm soil profile which show a systematic surface morphology variation with depth. In the profile, we observed a transition from angularly-pitted surfaces to rounded surfaces at a depth between 60 and 80 cm, suggesting that the critical Si concentration is reached in the permeating fluids at that point. We suggest that the observation of etch features on these low- temperature etched grains indicates that our high temperature work does have relevance to dissolution features formed under

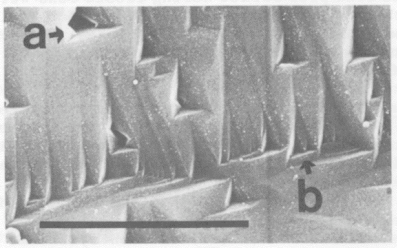

Figure 5. SEM photomicrograph of etch tubes (a) and terraced etch pits (b) on sample R5S5SE etched 31.5 hours at 0.53 C_o. (Scale bar = 10 microns.)

different temperature conditions. The impurity content of the quartz and the solution may also affect etching. If so, natural etching may give clues to the saturation index and the impurity content of paleo-fluids.

Several refinements of our experiments could test these theories further. By measuring etch pit densities as well as pit dimensions on sequentially-etched crystals, nucleation rate data and pit growth data could be collected, yielding information about the rate-limiting steps and mechanisms of dissolution. In addition, since the critical concentration is extremely dependent on surface energy of the crystal-water interface (Equation 4), careful measurement of C_{crit} yields a precise measurement of γ. Our data indicates an interfacial energy of 280 $\pm$ 90 mJm^{-2} for Arkansas quartz at 300°C, which compares well with Parks' value of 360 mJm^{-2} for 25°C (10). Similar experiments on other minerals could provide essential surface energy data.

Whether etch pit formation is important in determining dissolution kinetics and controlling the general reactivity of a crystal will depend on the nature of different crystals, as well as the overall dislocation density. Normally, crystal edges are a ready source of ledges for crystal dissolution. At low concentrations ($C < C_{crit}$), crystals will dissolve at edges, steps, cracks, etc., as well as at nucleated pits in both perfect and imperfect crystal. The fastest of these parallel processes should be rate-determining. If dislocation density is large enough, or if dissolution from edges is slow enough, etch pit dissolution may make a major contribution to the rate of bulk dissolution and be rate-determining. In this case, these minerals would show a change in rate-limiting step as C rises above C_{crit} and dissolution at dislocations slows.

Wintsch and Dunning (8) calculated that the solubility of plasticly deformed quartz in water should not be significantly higher than the ideal equilibrium value. However, enhanced dissolution at dislocations could significantly increase the dissolution

rate. This enhanced reactivity would be important in determining rates of mass transfer in zones of intense deformation. We are currently conducting dissolution kinetics experiments with such deformed material.

Formation of etch pits on naturally-weathered mineral surfaces has been noted by many workers (28-30). A theory based on laboratory etching experiments (31,32) has suggested that, for feldspars, surface layer buildup in etching holes may explain non-congruent dissolution (33). Recent evidence from Holdren and Speyer (34) has also shown that the dissolution rate of feldspar is not always directly proportional to surface area, but may instead be proportional to active site concentration. These results seem to imply that etch pit formation may be a rate-controlling step in feldspar dissolution under some conditions. In order to generalize laboratory dissolution rates for these materials to natural weathering processes, it may be necessary to measure natural defect densities. However, the reproducibility of dissolution rates for fluorite and calcite in our laboratory (35 and unpublished data) and for quartz (22) indicates that presumed differences in dislocation etch pit density does not affect the dissolution kinetics of these minerals within a factor of $\pm$10%. This could be explained by assuming that laboratory samples have dislocation densities which are equal to within $\pm$ 10%, or that laboratory preparation techniques produce equivalent dislocation densities. Alternatively, these observations could imply that etch pit contribution to overall bulk dissolution rate for these minerals is minimal.

To further understand and model bulk dissolution of minerals, careful experiments such as we have discussed above will be necessary. Dislocation etch pits, as sources of ledges on a surface, provide good control in measuring ledge or kink velocities. Work in this area, applied to geologically important minerals, will extend our understanding of the rates and mechanisms of alteration reactions. In addition, our soil profile work suggests that there may be information recorded on mineral surfaces which will be useful in reconstructing flow, compositional, and temperature histories of paleo-fluids.

Legend of Symbols

a	thickness of one molecular layer of quartz
A	frequency factor
b	Burger's vector of dislocation
C	concentration
C_{crit}	critical concentration
C_o	equilibrium concentration
g	chemical affinity per unit volume
ΔG	free energy of formation of a pit at a dislocation
ΔG^*	activation barrier toward formation of pit of critical radius on surface
J	pit nucleation rate
r	radius of pit
r_o	dislocation core radius
R	gas constant
T	temperature

v_n	dissolution rate in a direction normal to the surface
v_s	dissolution rate in a direction parallel to the surface
$\bar{V}$	molar volume
X_d	fraction of surface sites intersected by dislocations
γ	interfacial energy
τ	shear modulus
ν	Poisson's ratio

Acknowledgments

This work was funded by NSF grant #EAR-82-18726 and #EAR-84-19421. The soil profile analysis and much of the hydrothermal work was completed by S.R. Crane as her senior thesis at Princeton University. Maria Borscik, Elaine Lenk, and Laurel Pringle-Goodell helped with chemical, SEM and TEM analyses. D.A.C. gratefully acknowledges support from the Shell Companies Foundation and R.F.S. acknowledges support from the Venezuelan Ministerio del Ambiente y Recursos Naturales Renobales, a Dusenbery Preceptorship, and N.S.F. grant #EAR 84-07651.

Literature Cited

1. Frank, F.C. Acta Cryst. 1951, 4, 497.
2. Cabrera, N.; Levine, M.M.; Plaskett, J.S. Phys.Rev. 1954, 96, 1153.
3. Cabrera, N.; Levine, M.M. Phil. Mag. 1956, 1, 450.
4. Sears, G.W. J. Chem. Physics 1959, 32, 1317.
5. Gilman, J.J.; Johnston, W.G.; Sears, G.W. J. Appl. Physics 1958, 29, 747.
6. Ives, M.B.; Hirth, J.P. J. Chem. Phys. 1960, 33, 517.
7. Lasaga,A. 4th Int. Symp. Water-Rock Inter. Ext. Abstr.,1983, p.269.
8. Wintsch, R.P.; Dunning, J. J. Geophys. Res. 1985, 90, 3649.
9. Heinisch, H.L. Jr.; Sines, G.; Goodman, J.W.; Kirby, S.H. J. Geophys. Res. 1975, 80, 1885.
10. Parks, G.A. J. Geophys. Res. 1984, 89, 3997.
11. Hirth, J.P.;Pound, G.M. "Condensation and Evaporation: Nucleation and Growth Kinetics", MacMillan Co.: New York, 1963.
12. Johnston, W.G. Prog. Ceram. Sci. 1962, 2, 3.
13. Joshi, M.S.; Vag, A.S. Sov. Phys.Cryst. 1968, 12, 573.
14. Joshi, M.S.; Kotru, P.N.; Ittyakhen, M.A. Sov. Phys. Cryst. 1960, 15, 83.
15. Crerar, D.A.; Axtmann, E.V.,; Axtmann, R.C. Geochim. Cosmochim. Acta 1981, 45, 1259.
16. Brantley, S.L.; Crane, S.R.; Crerar, D.A.; Hellmann, R.; Stallard, R. Geochim. Cosmochim. Acta, in press.
17. Hicks, B.D. Masters Thesis, University of Missouri-Columbia, Missouri, 1985.
18. Walther, J.V.; Helgeson, H.C. Amer. Jour. Science 1977, 277, 1315.
19. Fournier, R.O.; Potter, R.W. Geochim. Cosmochim.Acta 1982, 46, 1969.

20. Crane, S.R. Senior Thesis, Princeton University, Princeton, New Jersey, 1985.
21. Stallard, R.F. In "The Chemistry of Weathering"; Drever, J.I., Ed.; NATO ASI SERIES vol. 149, D. Reidel PublishingCo.: Dordrecht, 1984, pp.293-316.
22. Rimstidt, J.D.; Barnes, H.L. Geochim.Cosmochim.Acta 1980,44, 1683.
23. Nielsen, J.W.; Foster, F.G. Am. Mineral. 1960, 45, 299.
24. Joshi, M.S.; Kotru, P.N.; Ittyachen, M.A. Am. Mineral. 1978, 63, 744.
25. Holdren, G.R.; Speyer, P.M. Geochim. Cosmochim. Acta 1985, 49,675.
26. Stein, C.L. Chem. Geology, in press.
27. Lasaga, A.C.;Blum, A.E. Geochim. Cosmochim. Acta, in press.
28. Wilson, M.J. Soil Sci. 1975, 119, 349.
29. Berner, R.A. Am. Jour. Sci., 1978, 278, 1235.
30. Velbel, M.A. In "Environmental Geochemistry"; Fleet, M.E., Ed.; MAC SHORT COURSE HANDBOOK Vol. 10, Mineralogical Society of Canada: Toronto, 1984, pp. 67-111.
31. Chou, L.; Wollast, R. Geochim. Cosmochim. Acta, 1984, 48,2205.
32. Holdren,G.R.; Speyer,P.M. Am. Jour. Sci., 1985, 285, 994.
33. Berner, R.A.; Holdren, G.R.; Schott, J. Geochim. Cosmochim. Acta 1985, 49,1657.
34. Holdren, G.R.; Speyer, P.M. Geochim. Cosmochim. Acta 1985, 49, 675.
35. Posey-Dowty, J., Crerar, D.A., Hellmann, R., and Chang, C.D. Am. Mineral. 1986, 71, 85.

RECEIVED August 4, 1986

Reprinted from ACS SYMPOSIUM SERIES No. 323
Geochemical Processes at Mineral Surfaces
James A. Davis and Kim F. Hayes, Editors